Available online www.jocpr.com

Journal of Chemical and Pharmaceutical Research, 2012, 4(4):1983-1989

Research Article

ISSN : 0975-7384
CODEN(USA) : JCPRC5

Structural and optical properties of Mg doped ZnO nanoparticles

R. Viswanatha, Y. Arthoba Nayaka *, C. C. Vidyasagar and T. G. Venkatesh

Department of Chemistry, School of Chemical Science, Kuvempu University, Shankaraghatta, India

---

ABSTRACT

Mg-doped ZnO have considerable interests owing to their unique optical, thermal and structural properties. ZnO and Mg doped ZnO nanoparticles with different doping concentration were prepared by precipitation method. The effect of Mg doping on the crystal structure, morphology and optical properties of the nanoparticles was also investigated. In this paper, we report the Synthesis of Mg-doped ZnO nanoparticles successfully with diameters ranging from 60 to 90nm via precipitation method. The surface morphology of synthesized material was investigated by using scanning electron microscope (SEM). The structure and phases of Mg-ZnO were analyzed by powder X-ray diffraction (XRD) method and the optical properties were measured by using UV–Vis spectrophotometer and photoluminescence spectroscopy.

Keywords: Mg doped ZnO; Nanoparticle; Precipitation; PL spectra; Powder XRD.

INTRODUCTION

As nanotechnology progresses and complex nanosystems fabricated, a rising impetus is being given to the development of multi-functional and size-dependent materials. Recent developments in nanoscience and nanotechnology have brought potential building blocks for a noscale electronic, optoelectronics, medicines and solar cells [1-4]. The surface/volume ratio increases as the material dimension decreases to nano-order. The high surface/volume ratio of nanomaterials has significant implications with respect to energy storage density.

Nanomaterials, especially metal oxides have received a considerable attention over the last few years due to their distinguished performance and potential applications in various fields. Among these oxides, ZnO exhibits the most diverse and abundant configurations of nanostructures [5-7]. ZnO is considered to be one of the best metal oxides that can be used at a nanoscale level. ZnO itself has normally a hexagonal or wurtzite structure and it is well-known as an n-type II–VI semiconductor with a wide direct band-gap of about 3.37 eV and a large exciton binding energy of 60 meV [8]. They have many applications in solar cells, luminescent, electrical and acoustic devices, chemical sensors, catalysis, electronics, gas sensor devices, optoelectronics, transducers, and biomedical devises [9,10]. Numerous applications have made the ZnO as wonder material for material scientists and the quantity of ZnO used in different application is also increasing. Hence, its production is ever increasing and a suitable method for preparing ZnO possessing less operating cost, working at ambient temperature, less time with narrow size range and better properties is a challenge for scientists [11].

Meanwhile, doping with selective elements offers an effective method to enhance and control the electrical and optical properties of ZnO nanostructures, which is crucial for its practical application. ZnO doped with proper elements, such as Li, Al, Mn and Cr has been studied [12–14]. By doping with MgO, which has a wider band-gap

(7.3 eV) [15], the band-gap of ZnO can be modulated for the realization of light-emitting devices operating in a wider wavelength region. The ZnO nanostructures are also being used in several industrial applications such as medicine, gas sensors, varistors, etc. The availability of a rich genre of nanostructures makes ZnO as an important material [16-19]. The doping of ZnO with a metal could change its properties, doping with the Group II elements (Cd, Mg) may modulate the value of the band gap and increase the UV luminescence intensity [20].

Large number of methods for the synthesis of ZnO are reported in the literature, such as precipitation, microemulsion, non-microemulsion, ultrasonic radiation precipitation [21], microwave irradiation [22], mechanical milling[23], solution combustion, microwave-assisted solvothermal [24] and sol–gel methods [25]. Different physical methods such as pulse laser deposition, vapor phase transparent process, chemical vapor deposition, and vapor transparent deposition have been developed for the preparation of nano-ZnO[26-29]. To date, a number of research workers have reported the fabrication of nanostructured ZnO powders with spherical [30], rod-like [31], flower-like and sheet-like [32] structures. Only a few reports [33, 34] have involved the synthesis of porous ZnO through an oxalate intermediate by a chemical route. Therefore, the synthesis of ZnO and Mg doped ZnO nanopowders via precipitation method in presence of CTAB could be worthwhile investigating.

In this paper, we report the synthesis and characterization of ZnO and Mg doped ZnO nanopaerticles by precipitation method and its characterization by using XRD, SEM, UV-Vis, Thermal analysis and Photoluminescence spectroscopic methods.

EXPERIMENTAL SECTION

Zinc sulphate, Magnesium sulphates were procured from Loba chemicals (Mumbai, India). Sodium hydroxide and cetyltrimethylammonium bromide were procured from S.D. Fine-CHEM Ltd. (Mumbai, India). All the chemicals were of analytical grade and were used as received for the experiments. Double distilled water was used for preparation of solutions.

Synthesis of ZnO and Mg-ZnO nanoparticles: To prepare ZnO nanoparticles, 100 mL of 0.2 M NaOH was added drop-wise into a solution containing 100 mL of 0.1 M Zinc sulphate solution under constant stirring. About 10 mg of CTAB was added as capping agent which inhibits anomalous growth of magnesium hydroxide crystals during the course of precipitation. Then the resulting solution was kept at room temperature for three hours under constant stirring. The so obtained white precipitate was centrifuged, washed several times with distilled water and then with alcohol and dried at 80^{o}C in an oven for 5 hours. To prepare Mg doped ZnO with different concentration of Mg (0.015, 0.020 and 0.025 M), NaOH was added to a mixture of 0.1 M Zinc sulphate and Magnesium sulphate solution 0.015, 0.020 and 0.025 M and the same procedure was repeated. The obtained samples were calcined in air at 400^{o} C for 2 hours to get Mg doped ZnO nanoparticles.

The diffraction patterns for the prepared Mg-ZnO nanoparticles were recorded on X-ray diffractometer (PHILIPS-1710) equipped with Cu Kα radiation (λ= 0.154 nM) with a scan rate of 0.02^{o} S^{-1}. The average size of nanoparticles was determined by using Scherer equation which is given by,

$$D = \frac{K\lambda}{\beta \cos\theta}$$

where D is the diameter of the crystallite size, K is the shape factor (the typical value is 0.9), λ is the wavelength of incident beam, β is the broadening of the diffraction line measured in radians at half of its maximum intensity (FWHM), and θ is the Bragg's angle.

The surface morphology and elemental analysis of the prepared nanoparticles was analyzed by scanning electron microscope (SEM) fitted with an energy dispersive X-ray spectroscopy (EDAX) (JEOL JSM-840A). The sample was coated with gold using low voltage sputtering and then analyzed under SEM operating at a voltage of 20 kV.

A UV-VIS-NIR spectrophotometer (USB 4000, Ocean Optics– USA) was employed to measure the optical parameters. The photoluminescence spectroscopy (Horiba Jobinyvon, model Labram HR 300) was used to measure

the emission characteristics of doped and undoped ZnO nanoparticles. The PL spectra were investigated at room temperature using Helium-Cadmium laser (325 nm) with the slit size of 100 µ and D2 filter.

RESULTS AND DISCUSSION

XRD analysis

Fig. 1 shows the XRD pattern of MgO and Mg doped ZnO with different Mg concentration annealed at 400^0 C for 2 hours. Fig. 1a illustrates a typical XRD spectrum of ZnO nanoparticles prepared by the precipitation method. Seven major diffraction peaks were seen at 31.7, 34.6, 36.2, 47.6, 56.5, 62.9 and 68.0, which can be assigned to the diffractions from (100), (002), (101), (102), (110), (103) and (112) planes respectively, according to the data base in JCPDS card (No-780-0075) with the lattice parameters: a = 0.3253 nm, c = 0.5209 nm and space group P63mc. This revealed that the resultant nanoparticles were pure ZnO with a hexagonal structure.

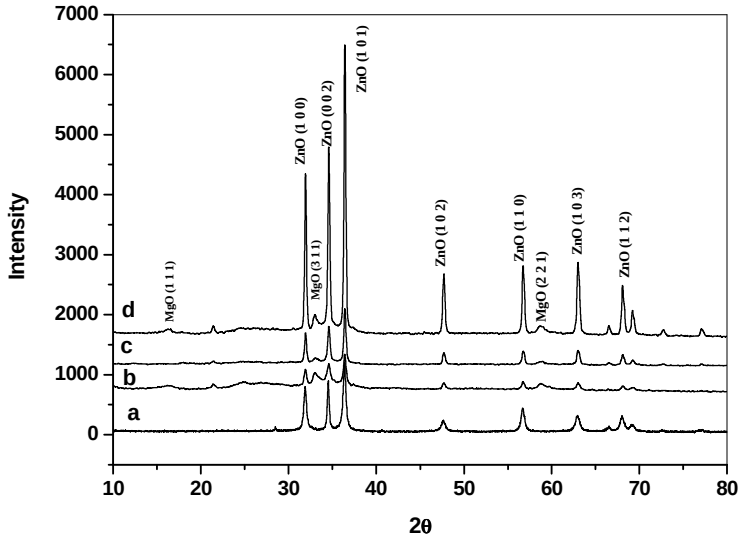

Fig. 1 XRD pattern of ZnO (a) and different concentrations 0.015 M (b), 0.020 M (c) and 0.025 M (d) of Mg doped ZnO nanoparticles calcined at 400^0C.

No impurities could be detected in this pattern, which implies hexagonal phase ZnO nanoparticles could be obtained under the current synthetic route. Fig. 1b, c and d depicts the XRD pattern of Mg doped ZnO with different Mg concentration of Mg (0.015, 0.02 and 0.025 M) annealed at 400^0 C. The diffraction peaks at 16.2, 32.6 and at 58.9 could be assigned to the diffractions from (111), (3100 and (221) planes respectively for Mg doped ZnO. The diffraction peak (101) was narrower than (100) and intern (100) peak was narrower than (002). This clearly indicated the presence of asymmetry in crystallite shape. The average crystalline size was calculated using Scherer equation and was found to be 86 nm for ZnO and 62, 76 and 88 nm fro Mg doped ZnO with different concentration of Mg (0.015, 0.02 and 0.025 M).

PL spectral analysis

Fig. 2A shows the room temperature photoluminescence spectra (PL) of ZnO nanoparticle and 2b shows the PL spectra of Mg doped ZnO nanoparticle. PL spectra were measured using He-Cd laser (325nm) as the excitation. The spectrum of ZnO includes a strong UV emission and a broad visible emission, corresponding to the near-band–edge (NBE) and the deep-level defects emission in ZnO structures [35, 36]. The NBE peak from ZnO has a small FWHM value at 379 nm. The spectra of Mg doped ZnO (2B) has an emission peak at 383 nm and a broad emission at 552 nm. Since the Mg doping decreased the band gap (Eg) and alternated the carrier concentration, the UV emission has a slight red-shift comparing with the emission peak of undoped ZnO. In addition, it shows a broad green emission peak centered around 549 nm which is usually observed for ZnO. The green emission peak is attributed to the defects present in ZnO crystals, such as vacancies and interstitials of zinc and oxygen. Compared with the undoped

ZnO, weaker green light emission at 552 nm and a small hump at 635 nm in Mg-doped structures might be related to lower oxygen vacancies in the samples. Mg doped ZnO structures have changed the optical properties significantly.

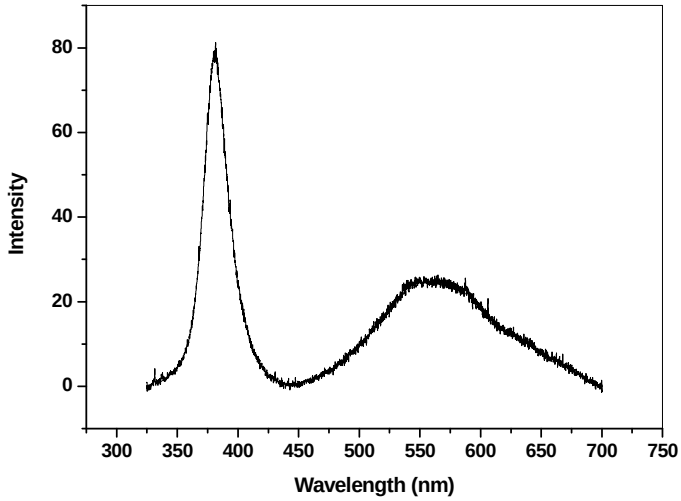

Fig. 2A

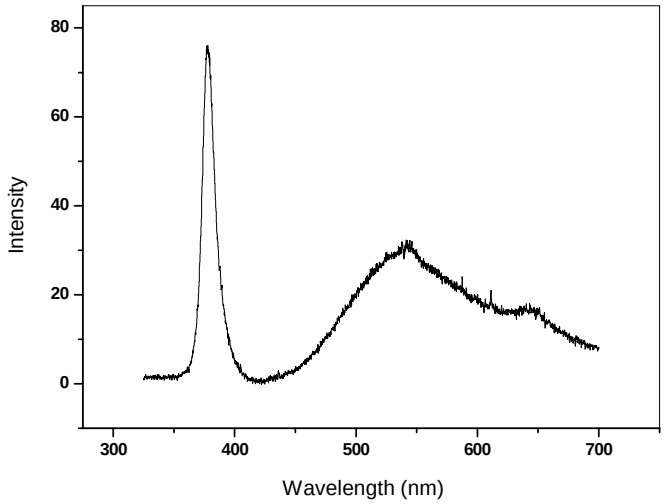

Fig. 2B

Fig. 2 Photoluminescence spectra of ZnO (2A) and Mg (0.015 M) doped ZnO (2B) nanoparticle.

FESEM analysis

The surface morphological properties of the nanoparticles were analyzed by using FESEM. Fig. 3a shows the scanning electron microscope pattern of ZnO nanoparticle and 3b, 3c and 3d shows the SEM pattern of Mg doped ZnO with the different concentrations of Mg (0.15, 0.20 and 0.25 M). The shape of ZnO nanoparticle obtained is granular and well dispersed. Sometimes the surface properties of ZnO are influenced from the incorporation of dopant. Especially the amount and kind of dopant can play an important role on the surface properties. The Mg doped ZnO nanoparticles are flake like structures and inhomogeneous in nature. This may be due to the defects

created by Mg doping. As the dopant concentration increases from 0.015 to 0.025 M the agglomeration of particles tales place and hence particle size increases.

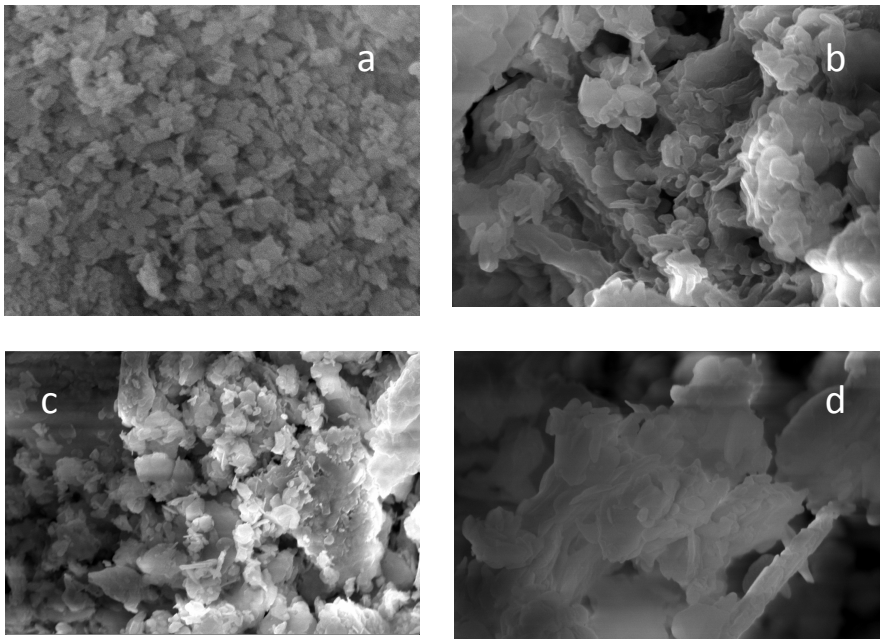

Fig. 3 FESEM pattern of ZnO (a) and different concentrations 0.015 M (b), 0.020 M (c) and 0.025 M (d) of Mg doped ZnO nanoparticles

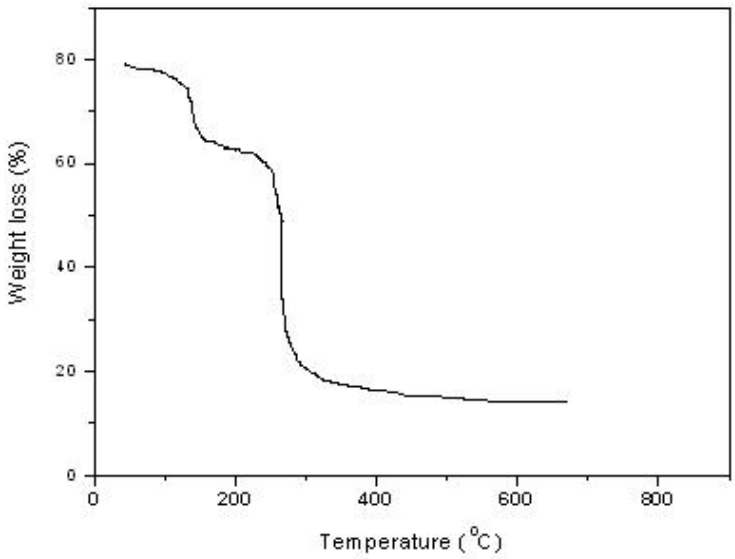

Fig. 4 Thermo gravimetric analysis of 0.1 M ZnO nanoparticle.

Thermal analysis

Thermal behavior of as-prepared sample was verified by the thermogravimetric analysis and the result is presented in Fig. 4. The TGA curve showed two weight losses. The first weight loss occurred at temperature between 120 and 180 ^{0}C, corresponded to the loss of surface adsorbed water molecules. The second weight loss appeared at 300 to 330 ^{0}C indicated major weight loss, suggesting that the precursor associated with decomposable $Zn(OH)_2$. The decomposition reaction may be represented as:

$ZnO\ H_2O \longrightarrow ZnO + H_2O$

$Zn(OH)_2 \longrightarrow ZnO + H_2O$

UV-Vis spectroscopy studies

Fig. 5 shows the UV-Vis spectra of ZnO and Mg doped ZnO nanoparticle obtained by precipitation method. ZnO shows the absorption peak at 361 nm (5a) and the Mg doped ZnO nanoparticles with different concentrations of Mg (0.015, 0.020 and 0.025 M) shows the absorption peaks at 363 (5b), 368 (5b) and 371 nm (5c) respectively. The small shift in the absorption band is attributed to the doping of Mg into ZnO. The band gaps (E_g) of ZnO and Mg-ZnO were calculated by using the formula $E = hc/\lambda$, where h is plank's constant, c is the velocity of light and λ is the wavelength. The band gap of ZnO was found to be 3.41 eV and Mg doped ZnO for different concentrations of Mg (0.015, 0.020 and 0.025 M) were found to be 3.39, 3.36 and and 3.34 eV nm respectively. With increase in the Mg concentration from 0.015 to 0.025 M, the optical absorption edge slightly shifts towards the longer wavelength region which may be attributed to the increase in the grain size.

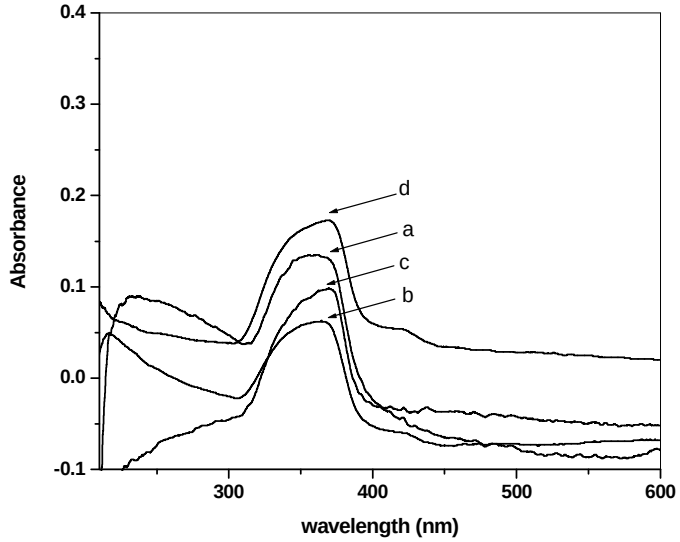

Fig. 5 UV-Vis spectra of ZnO (A) and different concentrations of Mg doped 0.015 M (b), 0.020 M (c) and 0.025 M (d) ZnO nanoparticles

CONCLUSION

In the present work, ZnO and Mg doped ZnO nanoparticles with different dopant concentration were prepared by simple precipitation method. The Mg doped ZnO nanoparticles have got the particle size in the range 60 to 90 nm. As the Mg concentration increases the agglomeration takes place and absorption edge slightly shifts towards the longer wavelength region which may be attributed to the decrease in band gap. The Mg doped nano particles have changed the optical properties effectively which was confirmed by PL spectroscopy.

REFERENCES

[1] Dinh TV. Nanotechnology in biology and medicine: methods, devices, and applications. CRC Press Taylor & Francis Group; **2007**.
[2] G L Hornyak, J Dutta, Fundamentals of nanotechnology. CRC Press Taylor & Francis Group; **2008**.
[3] Jai Singh, M.S.L. Hudson, S.K. Pandey, R.S. Tiwari, O.N. Srivastava. *Int J Hydrogen Energ*, **2012**, 37, 3748-3754.
[4] Sachin. V. Bangale*, R. D. Prashale and S. R. Bamane. *J. Chem. Pharm. Res*., **2011**, 3(6), 527-535
[5] PR Andres, JD Bielefeld, JI Henderson, DB Janes, VR Kolagunta, PC Kubiak, JW Mahoney, GR Osifchin, *Science*, **1996**, 273, 1690–1693.
[6] P.V. Kamath, J Phys Chem, **2002,** B106, 7729–7744.
[7] Afshin. Farahbakhsh, Hassan Ali Zamani, *J. Chem. Pharm. Res*. **2011**, 3(4), 381-388

[8] S. Suwanboon, A. Amornpitoksuk, A. Haidoux, J.C. Tedenac, *J. Alloys Compd*., **2008**, 462, 335.
[9] JX Wang, XW Sun, A Wei, Y Lei, XP Cai, CM Li, ZL Dong, Appl Phys Lett, **2006**, 88, 233106(1–3).
[10] S Arivoli; M Hema; S Parthasarathy; N Manju. *J. Chem. Pharm. Res*. **2010**, 2, 626.
[11] K. G. Chandrappa, T.V. Venkatesha, K. Vathsala, C. Shivakumara. *J Nanopart Res*, **2010**, 12(7), 2667-2678
[12] Y. Liu, J.H. Yang, Q.F. Guan, L.L. Yang, Y.J. Zhang, Y.X.Wang, B. Feng, J. Cao, X.Y. Liu, Y.T. Yang, M.B.Wei, *J. Alloys Compd*., **2009**, 486, 835.
[13] D.Y.Wang, J. Zhou, G.Z. Liu, *J. Alloys Compd*., **2009**, 481, 802.
[14] J.Wang,W. Chen, M.R.Wang, *J. Alloys Compd*. **2008**, 449, 44.
[15] L. Kumari,W.Z. Li, Charles H. Vannoy, Roger M. Leblanc, D.Z.Wang, *Ceram. Int*., **2009**, 35, 3355.
[16] Xia Y, Yang P, Sun Y, Wu Y, Mayers B, Gates B, et al. *Adv Mater*., **2003**, 15, 353.
[17] Kumar N, Dorfman A, Hahm, *J. Nanotechnology*, **2006**, 17, 2875.
[18] Sun ZP, Liu L, Zhang L, Jia DZ. *Nanotechnology*., **2006**, 17, 2266.
[19] PK Baskaran; BR Venkatraman; M Hema; S Arivoli. *J. Chem. Pharm. Res*. **2010**, 2, 642
[20] A Ohotomo, M Kawasaki, T Koida, K Masubuchi, H Koinuma, Y Sakurai, et al. *Appl Phys Lett*., **1998**, 72, 2466.
[21] C Sihai, R Xinmin, *Acta Phys Chim Sin*, **1999,** 11(2), 171–174.
[22] W Wenliang, L Dongsheng, H Xiangyang, S Zhenmin, W Jiwu, Z Caihua, *Chem Res Appl* **2001**. 13(2), 157–159.
[23] K .J Rao, Krishnamurthy Mahesh and Sundeep Kumar, *Bul Mater Sci*, **2005**, 28, 19–24.
[24] HM Deng, J Ding, Y Shi, XY Liu, J Wang, *J Mater Sci*, **2001**, 36, 3273–3276.
[25] M Vafaee, MS Ghamsari, *Mater Lett*, **2007**, 61, 3265–3268.
[26] Y Nakata, T Okada, M Maeda, Appl Surf Sci, **2002**, 197, 368–370.
[27] YZ Yoo, ZW Jin, T Chikyow, T Fukumura, M Kawasaki, H Koinuma, *Appl Phys Lett*, **2002**, 81, 3798-3800.
[28] BJ Chen, XW Sun, Xu CX, BK Tay, *Phys E*, **2004**, 21, 103–107.
[29] YJ Li, R Duan, PB Shi, GG Qin, *J Cryst Growth*, **2004**, 260, 309–315.
[30] Y. Zhang, Y. Liu, L. Wu, H. Li, L. Han, B. Wang, E. Xie, *Appl. Surf. Sci*, **2009**, 255, 4801-4805.
[31] A. Ishizumi, Y. Takahashi, A. Yamamoto, Y. Kanemitsu, *Mater Sci Eng B*, **2008**, 146, 212-215.
[32] Q. Xiao, S. Huang, J. Zhang, C. Xiao, X. Tan, *J. Alloys Compd*., **2008**, 459, L18-L22.
[33] K.G. Kanade, B.B. Kale, R.C. Aiyer, B.K. Das, *Mater. Res. Bull.*, **2006**, 41(3), 590-600.
[34] Z. Jia, L. Yue, Y. Zheng, Z. Xu, *Mater. Chem. Phys*., **2008**, 107(1), 137-141.
[35] D.C. Reynolds, D.C. Look, B. Jogai, T.C. Collins, *Appl. Phys. Lett*. **2001**, 79, 3794-3796.
[36] Boemare, T. Monteiro, M.J. Soares, J.G. Guilherme, E. Alves, *Physica B*, **2001**, 308, 985-988.